A&A 385, L1–L4 (2002)
DOI: 10.1051/0004-6361:20020233

Astronomy & Astrophysics

Submilliarcsecond-resolution mapping of the 43 GHz SiO maser emission in the bipolar post-AGB nebula OH231.8+4.2⋆

C. Sánchez Contreras[1,2], J. F. Desmurs[1], V. Bujarrabal[1], J. Alcolea[1], and F. Colomer[1]

[1] Observatorio Astronómico Nacional (OAN), Apdo. 1143, 28800 Alcalá de Henares, Spain
e-mail: sanchez,bujarrabal,desmurs,j.alcolea,colomer@oan.es
[2] Jet Propulsion Laboratory, California Institute of Technology, MS 183-900, 4800 Oak Grove Dr., Pasadena, CA 91109
e-mail: sanchez@eclipse.jpl.nasa.gov

Received 30 November 2001 / Accepted 11 February 2002

Abstract. We present ∼0.3 milliarcsec-resolution maps of the SiO ($v = 2$, $J = 1{-}0$) maser emission in the bipolar post-AGB nebula OH 231.8+4.2 obtained with the Very Long Baseline Array. These observations have provided for the first time the structure and kinematics of the close stellar environment in a proto-Planetary Nebula. Our observations reveal the SiO maser emission arising in several bright spots of less than $\sim 10^{13}$ cm in size forming a structure elongated in the direction perpendicular to the symmetry axis of the nebula. Such a distribution is consistent with an equatorial torus with a radius of ∼6 AU around the central star. A complex velocity gradient is found along the torus, which suggests rotation and infall of material towards the star. The rotation and infalling velocities deduced are of the same order and range between ∼7 and ∼10 km s^{-1}. From our data, we estimate the mass of the SiO torus and the central star, as well as a stringent upper limit to the present stellar mass-loss rate.

Key words. masers – stars: AGB and post-AGB – stars: mass-loss – circumstellar matter – stars: individual: OH231.8+4.2 – stars: variables: general

1. Introduction

In contrast to the circumstellar envelopes around Asymptotic Giant Branch (AGB) stars, the subsequent evolutionary stage of proto-Planetary and Planetary Nebulae (PPNe & PNe) show conspicuous asymmetries and collimated winds whose origins are not yet well understood. To explain the evolution of post-AGB objects from spherical AGB envelopes, several models have postulated the presence of dense rings or disks close to the central star (see e.g. Frank 1999, for a review): these disks would be the main agents of the collimation and acceleration of the stellar wind. However, these inner equatorial disks have not been observed up to now.

OH 231.8+4.2 (hereafter OH 231.8) is a well studied but puzzling PPN: it is composed of a remarkable bipolar nebula that shows all the signs of post-AGB evolution, namely, bipolar outflows with velocities up to ∼400 km s^{-1}, shock-excited gas, shocked chemistry, etc., and, at least, one red star (an M 9 III Mira variable) (see Alcolea et al. 2001, and references therein). The unusual presence of a late-type star in the core of a post-AGB nebula (PPN's central stars are typically hotter, with spectral types from B to K) allows the SiO circumstellar masers to survive at a few stellar radii, providing a unique tool for studying the stellar neighborhood in an object with bipolar outflows. Previous observations of the 86 GHz SiO masers show regular variations with time of the line intensity and profile consistent with the period of the NIR light-curve, ∼700 d (Sánchez Contreras et al. 2000a; Kastner et al. 1992). This variability is attributed to the pulsation of the Mira inside OH 231.8.

2. Observations and results

We have mapped, with submilliarcsec resolution, the SiO maser emission in OH 231.8 (RA = $07^{\rm h}42^{\rm m}16^{\rm s}.93$, Dec = $-14°42'50''.2$, J2000). Observations were carried out on 2000 May 14 using nine antennas of the Very Long Baseline Array (VLBA). We simultaneously observed the $v = 1$, $J = 1{-}0$ (43.122 GHz) and $v = 2$, $J = 1{-}0$ (42.820 GHz) SiO maser transitions, but only the latter (more intense) was detected. Data were recorded in dual circular polarization with one 4 MHz (27.8 km s^{-1}) band.

Send offprint requests to: C. Sánchez Contreras,
e-mail: sanchez@eclipse.jpl.nasa.gov

⋆ Based on observations with the Very Large Baseline Array of the The National Radio Astronomy Observatory (NRAO). NRAO is a facility of the National Science Foundation operated under cooperative agreement by Associated Universities, Inc.

In principle, all four Stokes parameters could be retrieved from the data, but due to some problems in the detection of polarization in one of the calibrators, the polarization maps are not reliable. The correlation of the data was performed at the NRAO in Socorro, New Mexico (USA), producing 128 channel auto and cross-correlation spectra with channel spacing of 31.25 kHz (0.2 km s^{-1}). Data were calibrated using standard procedures within the Astronomical Image Processing System (AIPS) software package. The restored clean beam has full width at half maximum $\sim$0.6 $\times$ 0.16 milliarcsec (mas) and is oriented at a position angle PA = $-15°$. The total size and noise of the maps are 50 $\times$ 50 mas and $\sim$40 mJy/beam, respectively.

The observational results are displayed in Fig. 1: at the top we show the (auto- and cross-correlated) SiO $v = 2$, $J = 1{-}0$ maser profile and, at the bottom, the map of the integrated intensity over the different spectral channels. The LSR velocity of the spots is indicated in km s^{-1} units on the SiO flux map. The profile of the cross-correlated SiO maser line is formed by two narrow ($\sim$2–3 km s^{-1}) features centered at $\sim$30 and 41 km s^{-1}. The systemic velocity is $\sim$33 km s^{-1}, as deduced from mm-wave and optical spectroscopy (Sánchez Contreras et al. 2000a,b). The velocity of the maser spikes does not coincide with those observed for the same transition in 1983–1984, at $\sim$33, 26.5 and 28.5 km s^{-1} (Jewell et al. 1991), suggesting that the maser originates in a region with an unstable structure and/or kinematics. The differences between the auto- and cross-correlated SiO spectra indicate flux loses of $\sim$60%, which means that a more extended maser emission component is missed by the interferometer.

The SiO $v = 2$, $J = 1{-}0$ integrated flux map show the maser arising from several compact spots distributed in a elongated region which extents $\sim$8 mas (Fig. 1). Considering the distance to OH 231.8, $d \sim 1500$ pc (Bowers & Morris 1984; Kastner et al. 1992), the size of the clumps is $\lesssim 10^{13}$ cm. Such a clumpy distribution is typically found in late-type stars (Diamond et al. 1994; Desmurs et al. 2000) and is partially due to circumstellar inhomogeneities and the maser effect itself. The total extent of the maser emitting region is only $\sim$12 AU. This region is oriented perpendicular to the symmetry axis of the nebula, at PA = 21°, and shows complex kinematics. The easternmost group of spots (red-shifted, $\sim$40 km s^{-1}) shows a clear velocity gradient: the projected velocity increases $\sim$4 km s^{-1} from East to West (see a color velocity map in Fig. 1 of Desmurs et al. 2001). In the most intense and compact western spots (blue-shifted, $\sim$30 km s^{-1}) the velocity variation is smaller ($\Delta V \sim 2$ km s^{-1}).

3. Structure and kinematics of the OH 231.8 central star's vicinity

As expected, the SiO maser emission in OH 231.8 originates very close to the central star, presumably inside the dust condensation radius (beyond this point, $\gtrsim 5\,R_\star$, the gas-phase Si is almost totally depleted in dust grains, e.g. Greenhill et al. 1995). Considering the total luminosity

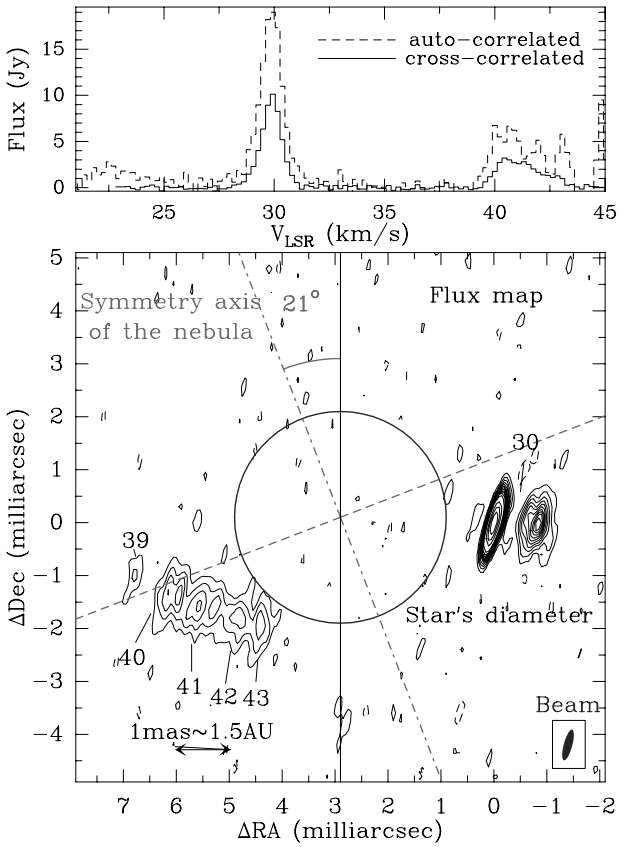

Fig. 1. Top) VLBA profile of the SiO $v = 2$, $J = 1{-}0$ maser line in OH 231.8. **Bottom)** Total intensity map of the SiO maser. The LSR velocity (km s^{-1}) of a number of maser spots is indicated ($V_{\rm sys} \sim 33$ km s^{-1}). The circle represents the angular extent of the OH 231.8 central Mira. The direction of the nebular symmetry axis and equator are indicated by dashed lines.

and temperature of the central Mira of OH 231.8, $L \sim 10^4\,L_\odot$ and $T_\star \sim 2300$ K, we deduce a mean stellar radius of $R_\star \sim 3$ AU, as expected for a Mira-type star (e.g. van Belle et al. 1996). Accordingly, the SiO $v = 2$, $J = 1{-}0$ emitting region is only at $\sim 2\,R_\star$ from the star, indicating that the maser originates almost in the stellar surface, in the so-called extended atmosphere. This region is expected to be turbulent and, in general, to show very complex kinematics involving in- and out-flowing motions depending on the stellar phase (Diamond et al. 1994).

The distribution of the SiO maser spots in OH231.8, orthogonal to the nebular symmetry axis, suggests the presence of an equatorial torus or disk surrounding the central star. Such a distribution is remarkably different from that found in other late-type stars, where the masers form a roughly spherical ring-like chain of spots resulting from tangential maser amplification in a thin, spherical shell (Diamond et al. 1994; Desmurs et al. 2000).

In the following, we explore the reliability of the torus scenario, since similar structures are invoked by post-AGB evolution theories. However, note that other more complex geometries cannot be ruled out from the present data

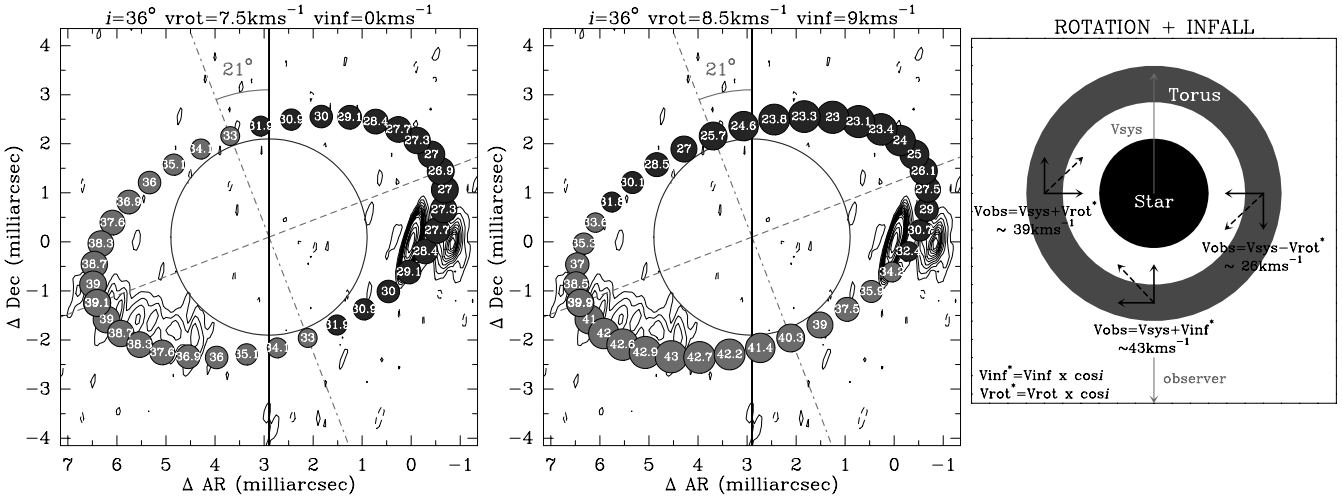

Fig. 2. Spatio-kinematical model of the SiO maser clumps in OH 231.8. In the model, the masers arise from an equatorial torus around the central star (right panel). The position and LSR velocity (in km s^{-1}) of the SiO maser spots predicted by the model assuming pure rotation (left) and rotation+infall (central) are indicated by the circles and numbers inside (black/grey colors are used for blue-/red-shifted spots). The model predictions are superimposed to the SiO $v = 2$, $J = 1{-}0$ integrated intensity map. The torus inclination, rotation and infall velocities assumed appear at the top of each panel.

(Sect. 4). We have constructed a spatio-kinematical model for the SiO maser emitting region and compared its results with our observations. In Fig. 2 (right) we show a sketch of the torus-like structure (as viewed from the nebula north-pole) and two velocity fields considered in the model. The expected distribution and LSR velocities of the maser spots for each kinematical model are superimposed on the flux map in the left panels.

Regarding the geometry, the observed maser distribution is compatible with a torus with radius $R \sim 6$ AU perpendicular to the nebular symmetry axis (inclined $\sim$36° with respect to the plane of the sky; Kastner et al. 1992). This torus-like structure is not totally traced by the maser spots, which are observed only at the edges. Such a distribution is expected, even for a homogeneous torus, if the maser is tangentially amplified (as for most late-type stars, see above). This amplification mechanism leads to the most intense maser features at the edges of the torus-like structure. Moreover, given the comparable size of the star and the maser emitting region, ocultation by the star of the torus rear is also likely, which would partially explain the small number of detected spots.

The kinematics in the equatorial torus is complex and at least two different components are required to explain the observed velocity gradient. The blue- and red-shifted maser features are west- and east-displaced, suggesting rotation with the east part of the torus receding from us. However, the velocity gradient found in the eastern SiO maser features cannot be reproduced only with pure rotation, which would lead to the largest velocities at the edges of the torus (see Fig. 2, left panel). The observed distribution of the velocity, decreasing towards the east, can be better explained if *rotation and infall* are present in the torus (Fig. 2, central panel). To fit the data, rotation and inflow velocities in the range 7–10 km s^{-1} are required, with the rotation velocity being slightly smaller than the infall velocity. For the assumed geometry, an expanding+rotating velocity field is not able to reasonably fit our data since the velocity in the torus would increase in the wrong direction as for the pure rotation case.

We finally note that all SiO maser profiles of OH 231.8 published to date (Jewell et al. 1991; Sánchez Contreras et al. 2000a, and references therein) show a few spikes spanning from $\sim$23 to 43 km s^{-1} (LSR). This shows that the gas velocities in the inner circumstellar envelope have never been much higher than at present.

4. Discussion

The SiO maser emission in OH 231.8 indicates densities of $\sim 10^9{-}10^{10}$ cm^{-3} at only $\sim$6 AU from the star. Such high densities (and temperatures of the order of $\sim$1000 K) are required to produce SiO maser emission in AGB envelopes (e.g. Lockett & Elitzur 1992; Bujarrabal 1994). The presence of dense material in the inner circumstellar envelope of this object is a clear indication that the mass-loss is going on. This is, on the other hand, consistent with the pulsating nature of the central Mira star. Since the SiO maser originates before the region of expansive kinematics (which takes place beyond the region of massive dust formation by radiation pressure on dust), the present mass-loss rate, $\dot{M}$, in OH 231.8 cannot be straightforwardly obtained as for an stationary outflow ($\dot{M} = 4\pi r^2 \rho V_{\rm exp}$). However, this procedure yields an upper limit for $\dot{M}$, since the density in the expanding envelope is expected to be smaller than in the innermost SiO maser emitting region. Accordingly, we derive $\dot{M} \ll 2 \times 10^{-5}\, M_\odot$ yr^{-1}, for an expansion velocity of $\sim$7 km s^{-1} (Sánchez Contreras et al. 2000a). This value is significantly smaller than the late-AGB mass-loss rate deduced from CO mapping ($\sim 1.6 \times 10^{-4}\, M_\odot$ yr^{-1}; Alcolea et al 2001), indicating that

the stellar mass-loss rate is presently much smaller than it was when the bulk of the nebula was ejected.

In our opinion, the structure traced by the SiO maser emission in OH 231.8, compatible with a rotating+infalling torus very close to the central star, is unlikely an accretion disk. In fact, the dramatic changes with time of the SiO $v = 2$, $J = 1{-}0$ profile suggest that the masers lie in a region with an unstable structure and/or kinematics, rather than in a stable accretion disk. Moreover, accretion disks are expected around the compact companion in a binary system and less likely around the mass-losing star. On the other hand, the mass of the SiO emitting region is only $\sim 2{\times}10^{-7}\,M_{\odot}$ (for the derived density and assuming a torus with $R \sim 6$ AU, and thickness and height $\sim 10^{13}$ cm). Even considering that the SiO spots probe only a small fraction of the total volume of the maser zone ($\sim$0.1%; Greenhill et al. 1995), with such a low mass, the observed torus would hardly be the collimating agent of the bipolar outflows in OH 231.8, which carry out a linear momentum of $\sim 27\,M_{\odot}$ km s^{-1} (Alcolea et al. 2001).

As an alternative to the accretion disk, the mass infall could be due to the pulsation of the central star. During the observations, the phase of the NIR/optical light-curve was $\sim$0.3 (Sánchez Contreras et al. 2000b), which is consistent with a phase of stellar contraction (Boboltz et al. 1997, and references therein).

Considering the rotation and infall velocities deduced from the data, we have estimated the mass of the central object. If the mass infall is due to pulsation, the typical radius variations during the pulsation in Mira stars (<40%, e.g. van Belle et al. 1996) yields a value for the mass of $M_{\star} \gtrsim 1\,M_{\odot}$. From the rotation velocity we derive $M_{\star} \sim 0.5\,M_{\odot}$ for a system in hydrostatic equilibrium. Since the clumps inflow indicate that gravity dominates over centrifugal forces, the previous figure has to be considered as a lower limit. The two values of the mass above are consistent with the difference between the main-sequence mass of the central star, $\sim 3\,M_{\odot}$ (Jura & Morris 1985) and the mass in the circumstellar envelope $\gtrsim 1\,M_{\odot}$ (Alcolea et al. 2001). This result suggests that the nebula in OH 231.8 primarily resulted from the central Mira mass-loss process.

Although the elongated structure traced by the SiO maser is unlikely the direct agent of wind collimation in OH 231.8 (which requires more massive disks; see Frank 1999), it may be, in some sense, connected to the remarkable bipolarity of this object (we recall that "normal" Miras show ring-like maser distributions). The toroidal geometry could have resulted from a) the interaction of fast jets (collimated by other means) with an initially isotropic AGB wind: the former would have opened two opposite holes in the spherical envelope, shaping a ring-like structure. The OH 231.8 torus could also indicate b) an originally aspherical stellar atmosphere. A number of binary and single-star processes have been proposed to explain equatorial density enhancements in evolved stars (Frank 1999). However, as far as we know, these models deal with regions farther away from the star than that probed by the SiO masers and, therefore, their results are not directly comparable to our data. Nevertheless, these mechanisms are expected to imprint some asymmetries also on the extended-atmosphere of the mass-losing star (for example, tidal deformation of the primary's surface due to the gravitational interaction with a companion is expected in binary systems; Mastrodemos & Morris 1999), although those effects are not quantitatively studied at present.

Although the rotating+infalling torus scenario is attractive (it may constitute the first hint of the inner disks postulated by theories to explain the onset of bipolarity in PPNe) and consistent with our observations, new SiO maser maps are needed to check its reliability. In fact, the small number of detected spots (probably because our observations were done close to a minimum of maser emission) does not allow us to characterize the geometry of the innermost regions of OH 231.8 without ambiguity. Since maser spots can appear and disappear during the stellar cycle (Diamond et al. 1994), we cannot rule out the presence of a more extended structure (not necessarily a torus) not totally visible at the time of our VLBA observations.

Acknowledgements. We are grateful to R. Sahai and A. Gil de Paz for critically reading this letter. We also thanks the referee, P. Diamond, for valuable comments. This work was performed at the Observatorio Astronómico Nacional (Spain), under Spanish DGES project PB96-0104, and at the Jet Propulsion Laboratory, California Institute of Technology, under a contract with the National Aeronautics and Space Administration.

References

Alcolea, J., Bujarrabal, V., Sánchez Contreras, C., Neri, R., & Zweigle, J. 2001, A&A, 373, 932
Boboltz, D. A., Diamond, P. J., & Kemball, A. J. 1997, ApJ, 487, L147
Bowers, P. F., & Morris, M. 1984, ApJ, 276, 646
Bujarrabal, V., 1994, A&A, 285, 953
Diamond, P. J., Kemball, A. J., Junor, W., et al. 1994, ApJ, 430, L61
Desmurs, J. F., Bujarrabal, V., Colomer, F., & Alcolea, J. 2000, A&A, 360, 189
Desmurs, J. F., Sánchez-Contreras, C., Bujarrabal, V., Colomer, F., & J. Alcolea 2001, Proceedings of the IAU Symp. No. 206 [astro-ph/0109543]
Frank, A. 1999, New Astron. Rev., 43, 31
Greenhill, L. J., Colomer, F., Moran, J. M., et al. 1995, ApJ, 449, 365
Jewell, P. R., Snyder, L. E., Walmsley, C. M., Wilson, T. L., & Gensheimer, P. D. 1991, A&A, 242, 211
Jura, M., & Morris, M. 1985, ApJ, 292, 487
Kastner, J. H., Weintraub, D. A., Zuckerman, B., et al. 1992, ApJ, 398, 552
Lockett, P., & Elitzur, M., 1992 ApJ, 399, 704
Mastrodemos, N., & Morris, M. 1999, ApJ, 523, 357
Sánchez Contreras, C., Bujarrabal, V., Neri, R., & Alcolea, J. 2000a, A&A, 357, 651
Sánchez Contreras, C., Bujarrabal, V., Miranda, L. F., & Fernández-Figueroa, M. J. 2000b, A&A, 355, 1103
van Belle, G. T., Dyck, H. M., Benson, J. A., & Lacasse, M. G. 1996, AJ, 112, 2147